

RESEARCH PAPER



Involvement of L-selectin expression in *Burkholderia pseudomallei*-infected monocytes invading the brain during murine melioidosis

Yao-Shen Chen^{a,b,†}, Hsi-Hsun Lin^{c,†}, Pei-Tan Hsueh^{d,e}, Wei-Fen Ni^e, Pei-Ju Liu^e, Pei-Shih Chen^{f,g}, Hsin-Hou Chang^h, Der-Shan Sun^h, and Ya-Lei Chen^{id}^e

^aDepartment of Internal Medicine, Kaohsiung Veterans General Hospital, Kaohsiung, Taiwan; ^bDepartment of Internal Medicine, National Yang-Ming University, Taipei, Taiwan; ^cSection of Infectious Disease, Department of Medicine, E-Da Hospital and University, Kaohsiung Taiwan; ^dDepartment of Biological Science, National Sun Yat-sen University, Kaohsiung, Taiwan; ^eDepartment of Biotechnology, National Kaohsiung Normal University, Kaohsiung, Taiwan; ^fDepartment of Public Health, College of Health Science, Kaohsiung Medical University, Kaohsiung, Taiwan; ^gInstitute of Environmental Engineering, National Sun Yat-sen University, Kaohsiung, Taiwan; ^hDepartment of Molecular Biology and Human Genetics, Tzu Chi University, Hualien, Taiwan

ABSTRACT

The development of neurologic melioidosis was linked to the elicitation of *Burkholderia pseudomallei*-infected L-selectin^{hi}CD11b⁺ BALB/c cells in our previous study. However, whether monocytic L-selectin (CD62L, encoded by the *sell* gene) is a key factor remains uncertain. In the present study, after establishing multi-organ foci *via* hematogenous routes, we demonstrated that *B. pseudomallei* GFP steadily persisted in blood, splenic, hepatic and bone marrow (BM) Ly6C monocytes; however, the circulating CD16/32⁺CD45^{hi}GFP⁺ brain-infiltrating leukocytes (BILs) derived from the blood Ly6C monocytes were expanded in BALB/c but not in C57BL/6 bacteremic melioidosis. Consistent with these results, 60% of BALB/c mice but only 10% of C57BL/6 mice exhibited neurologic melioidosis. In a time-dependent manner, *B. pseudomallei* invaded C57BL/6 BM-derived phagocytes and monocytic progenitors by 2 d. The number of Ly6C⁺CD62L⁺GFP⁺ inflamed cells that had expanded in the BM and that were ready for emigration peaked on d 21 post-infection. Hematogenous *B. pseudomallei*-loaded *sell*^{+/+}Ly6C monocytes exacerbated the bacterial loads and the proportion of Ly6C⁺GFP⁺ BILs in the recipient brains compared to *sell*^{-/-} infected Ly6C cells when adoptively transferred. Moreover, a neutralizing anti-CD62L antibody significantly depleted the bacterial colonization of the brain following adoptive transfer of *B. pseudomallei*-loaded C57BL/6 or BALB/c Ly6C cells. Our data thus suggest that Ly6C⁺CD62L⁺ infected monocytes served as a Trojan horse across the cerebral endothelium to induce brain infection. Therefore, CD62L should be considered as not only a temporally elicited antigen but also a disease-relevant leukocyte marker during the development of neurologic melioidosis.

ARTICLE HISTORY

Received 16 March 2016
Revised 7 August 2016
Accepted 30 August 2016



KEYWORDS

Burkholderia pseudomallei; L-selectin; Ly6C⁺CD62L⁺; neurologic melioidosis; Trojan horse

Introduction

The life-threatening disease melioidosis is a result of *Burkholderia pseudomallei* infection and is endemic in Southeast Asia and Northern Australia.¹ Human melioidosis is transmitted by inhalation, ingestion and subcutaneous inoculation.² Septic melioidosis is the most severe form, although the clinical spectra vary, ranging from chronic to acute, localized to systemic, and/or asymptomatic to symptomatic infections.³ Once *B. pseudomallei* infection is established at a localized site, the primary foci can perniciously progress to secondary microabscesses in multiple organs *via* hematogenous dissemination.^{4,5} Rarely, meningitis occurs during melioidosis in humans.⁶

The mechanism by which *B. pseudomallei* invades the tightly protected central nervous system (CNS) is unclear. The development of neurologic melioidosis has been suggested to result from the destruction of the blood-brain barrier (BBB) *via* inflammatory cytokine- or lipopolysaccharide (LPS)-mediated mechanisms.⁷ Following intranasal infection in an animal model, *B. pseudomallei* invades the CNS through the olfactory nerves or the trigeminal nerve root.^{8,9} However, *B. pseudomallei* is an intracellular pathogen that systemically persists in a variety of phagocytic and non-phagocytic cells for months or years.¹⁰ Irrespective of the initial infection route, the proposed mechanisms for the development of CNS infection after

CONTACT Ya-Lei Chen  dan1001@ms31.hinet.net  Biotechnology, National Kaohsiung Normal University, No. 62., Sheng-Chung Rd., Yen-Chao, Kaohsiung, 82444, Taiwan.

[†]These authors contributed equally to this work.

© 2017 Taylor & Francis

the establishment of primary foci include direct invasion of the BBB by the free bacteria *via* circulatory dissemination or the migration of infected cells, known as a Trojan horse, across endothelial layers.¹¹

Susceptible BALB/c and resistant C57BL/6 mice are typically used as models to study melioidosis progression.^{12–16} Several lines of evidence support the importance of leukocyte migration in contributing to the dissemination of melioidosis in both models. *B. pseudomallei* stimulates the maturation of BALB/c and C57BL/6 bone marrow-derived dendritic cells (BMDCs) *in vitro* and, *in vivo*, is internalized into dendritic cells (DCs) and thus systemically disseminates to the lymph nodes, lung, spleen and blood after footpad injection of C57BL/6 DC cells carrying *B. pseudomallei*.^{17,18} However, the maturation of BMDCs was significantly improved in BALB/c mice compared to C57BL/6 mice after exposure to *B. pseudomallei*.¹⁷ Neurologic signs are observed in susceptible BALB/c and resistant C57BL/6 mouse models, whereas the *B. pseudomallei* loads in the brain usually lag behind those in the spleen, liver, lung or lymph nodes in BALB/c mice.^{19,20} We previously reported that the intracellular persistence of *B. pseudomallei* in the BM occurs prior to the development of neurologic melioidosis.²⁰ After adoptive transfer, selectin-expressing CD11b leukocytes harboring *B. pseudomallei* trigger the accumulation of a number of meningeal neutrophils and monocytes near the cerebral superior sagittal sinus and increase bacterial loads in the brains of BALB/c mice.²⁰ However, the origins of the CNS-infiltrating cells involved in the delivery of intracellular *B. pseudomallei* during melioidosis remain unclear. Additionally, direct evidence supporting the migration of blood-circulating infected cells to the CNS *via* selectin gene-mediated transmigration is needed. In particular, studies in resistant C57BL/6 mice may reveal potential mechanisms against neurologic melioidosis.

CNS infection *via* a Trojan horse requires several sequential events, including the bacterial invasion of leukocytes, chemokine attraction, complementary cell adhesion molecule (CAM) expression on leukocytes and endothelial layers, and leukocyte transmigration.^{21,22} The migration of inflamed cells across endothelial cells decreases if mice are deficient in L-selectin, a leukocyte adhesion molecule.^{23,24} Selectin (CD62) is a lectin family of single-chain transmembrane CAMs that binds to sugar moieties. This protein family contains 3 members, namely, P-selectin (CD62P), E-selectin (CD62E) and L-selectin (CD62L), which are primarily expressed by platelets (CD62P and CD62E), endothelial cells (CD62E) and leukocytes (CD62L).²⁴ The cell surface expression of L-selectin and P-selectin on leukocytes and endothelial cells has been associated with inflammation.^{23,24} During

bacterial infection, following the attraction of the chemokines monocyte chemoattractant protein-1 (MCP-1, CCR2 ligand) and fractalkine (CX₃CR1 ligand) and an increase in L-selectin (CD62L) expression on the inflamed cells, the CD11b⁺Ly6C⁺CCR2⁺CD62L⁺ and CD11b⁺Ly6C⁺CX₃CR1⁺ subsets derived from the CD34⁺ (haematopoietic progenitor cell antigen) and CD115⁺ (colony-stimulating factor 1 receptor) progenitor cells are expanded in the BM and eventually released into circulation.²⁵ We hypothesized that if a Trojan horse exists, migration-mediated L-selectin expression in the inflamed BM cells that carry intracellular *B. pseudomallei* will play a key role in the development of neurologic melioidosis *via* leukocyte migration.

Materials and methods

Strains and plasmids

B. pseudomallei vgh07 was isolated from the blood of a melioidosis patient in Taiwan.²⁶ The Personal Information Protection Act (Taiwan) legally prohibits the linking of *B. pseudomallei* data to the private information of melioidosis patients. *B. pseudomallei* GFP (green fluorescence protein) derived from vgh07 was constructed using a previously described protocol.²⁰ Briefly, the plasmid pKNOCK (*norB-pfliC-gfp-cat*) was constructed using specific PCR products, including the *norB* gene (UQ47_12230) and *fliC* promoter (517 bp upstream of the coding region of UQ47_17285), which were amplified from the chromosome of *B. pseudomallei* vgh07.²⁷ The *gfp* gene was derived from the pUT-miniTn5-*gfp-tet* (AY364166) plasmid. For a tri-parental mating system, *E. coli* DH5 α *pir* pKNOCK (*norB-pfliC-gfp-cat*, Cm^r, Ap^s; 10⁹ CFU), *E. coli* pRK2013 (10⁹ CFU; Cm^s, Ap^s) and *B. pseudomallei* vgh07 (10⁹ CFU; Cm^s, Ap^r) were mixed and filtered onto a cellulose membrane (<0.45 μ m). After conjugation, *B. pseudomallei* GFP was observed by fluorescent microscopy (Eclipse 50i; Nikon, Shinjuku, Tokyo, Japan). The appropriate insertion in the GFP-expressing strains was confirmed by PCR, sequencing and Southern hybridization (data not shown). The final scheme used to construct *B. pseudomallei* GFP is shown in Fig. 1.

All experiments using viable *B. pseudomallei* were performed in an air flow-controlled lab (BSL III level), and the procedures were approved by the Institutional Biosafety Committee (NKNU, Taiwan).

Induction of mouse melioidosis

Wild-type BALB/c and C57BL/6 mice were purchased from the Animal Laboratory Center (Taipei, Taiwan).

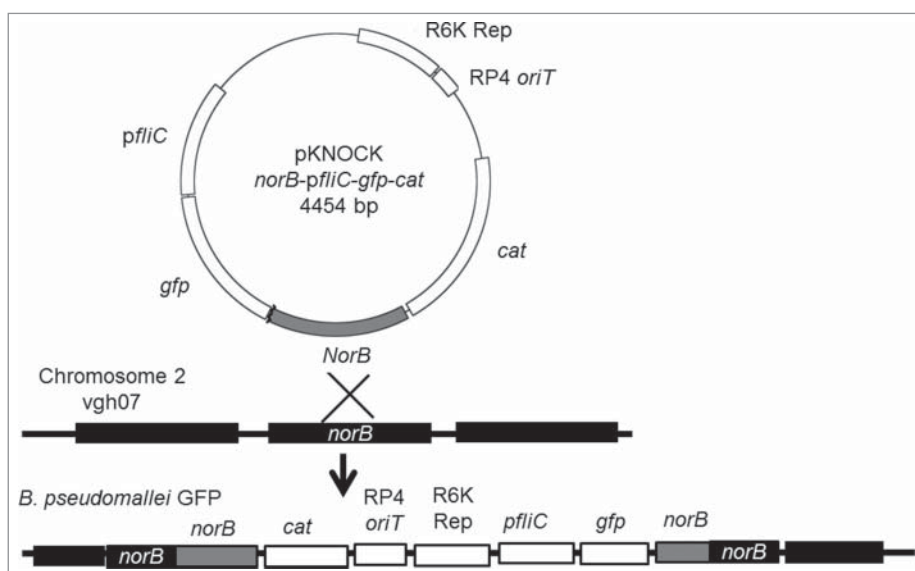


Figure 1. Construction of the integrated plasmid. The plasmid (pKNOCK *norB-pflIC-gfp-cat*) was designed as an integrated plasmid. After recombination, the integrated genes are inserted in chromosome 2 of *B. pseudomallei* vgh07.

Both *sell*^{-/-} (B6;129S2-Sellt1Hyn/J)²⁸ and *selp*^{-/-} (B6;129S2-Selptm1Hyn/J)²⁹ knockout (KO) C57BL/6 mice were obtained from The Jackson Laboratory, kindly provided by the Animal Center in Tzu Chi University through a material transfer agreement. Both the *sell*^{-/-} and the *selp*^{-/-} KO mice were backcrossed to the parental C57BL/6 strain for more than 6 generations. The KO mice were routinely checked for the specific amplicons for the *sell*^{-/-} (609 bp; forward primer, CAC GAC ACT AGT GAG ACG TC; reversed primer, GCA GTC CAT GGT ACC CAA CT), *sell*^{+/+} (1029 bp; forward primer, GGG AGC CCA ACA ACA AGA AG; reversed primer, GCA GTC CT GGT ACC CAA CT), *selp*^{-/-} (172 bp; forward primer, CTG AAT GAA CTG CAG GAC GA; revised primer, ATA CTT TCT CGG CAG GAG CA) and *selp*^{+/+} (forward primer, TTG TAA ATC AGA AGG AAG TGG; revised primer, AGA GTT ACT CTT GAT GTA GAT CTC C) genes from tail chromosomes.^{29,30} All animal experiments were conducted according to the Guide for the Care and Use of Laboratory Animals (National Animal Laboratory Center, Taiwan) and were approved by the Institutional Animal Care and Use Committee at the National Kaohsiung Normal University, Taiwan. To induce melioidosis, the mice (females, 8 weeks old) were intravenously infected with the indicated concentrations of *B. pseudomallei* GFP (100 μ L; 50 CFU [colony-forming units] for the BALB/c mice, 5×10^5 CFU for the C57BL/6 mice). The survival rates were recorded daily. The mice with melioidosis were sacrificed at the indicated times after infection to perform cytokine assays, cellular isolation, and histological examinations and determine bacterial loads in organs.

Histological examination

The mice with melioidosis were perfused with 100 mL of phosphate-buffered saline (PBS) *via* the heart. After perfusion, the skull was excised, fixed in 4% formaldehyde, de-calcified with 10% trichloroacetic acid, and processed for paraffin wax embedding using standard techniques.²⁰ The meningeal neutrophil infiltration and cerebral abscesses were observed using hematoxylin and eosin (H&E) stain. For the immunohistochemistry (IHC) assay, the primary antibodies were diluted in PBS according to the manufacturer's instructions and incubated with the sections (Table 1). Colorimetric detection of attached antibodies was performed using the UltraVision Quanto Detection System HRP Kit (Thermo Fisher Scientific Inc., Fremont, CA, USA) after adding Quanto Substrate. The antibody/polymer conjugate was visualized by applying DAB Quanto Chromogen (Thermo Fisher Scientific) dissolved in PBS to the tissue sections for 20 min. The intracellular *B. pseudomallei* GFP in a single-cell suspension were estimated using flow cytometry (see below) or imaged using confocal microscopy (FV500 Upright, BX60; Olympus Co., Shinjuku-ku, Tokyo, Japan).

Single-cell suspension

Single-cell suspensions were prepared from the spleen, BM, liver, and brain and peripheral blood cells of the mice with melioidosis at the indicated times after infection. Splenic mononuclear cell layers were separated by Ficoll-Hypaque (GE Healthcare Life Science

Table 1. Primary antibodies used for flow cytometry or immunohistochemistry in this study.

Target	Representative to	Conjugated ^a	Isotype control	Clone	Species	Concentration	Company
CD11b,	Leukocytes	PE-Cy7, PE or none	IgG2b κ	M1/70	Rat	2 μ g/mL	BD Pharmingen
Ly6C,	Monocytes	PE0Cy7, PE or none	IgM κ	AL-21	Rat	2 μ g/mL	BD Pharmingen
Ly6G,	Neutrophils	PE or none	IgG2a κ	1A8	Rat	2 μ g/mL	BD Pharmingen
F4/80,	Macrophages/Kupffer cells	PE or none	IgG2a κ	BM8	Rat	2 μ g/mL	BioLegend
CD3e,	T cells	none	IgG1 κ	145-2C11	Hamster	20 μ g/mL	BD Pharmingen
CD19	B cells	none	IgG2a κ	1D3	Rat	2 μ g/mL	BD Pharmingen
Bp ^b		none	IgG1	poly ^c	Rat	30 μ g/mL	Ref. (52)
CD45,	Leukocyte common antigens	PE	IgG2a κ	MEC13.3	Rat	2 μ g/mL	BD Pharmingen
CD16/32	Phagocytic cells	PE-Cy	IgG2b κ	2.4G2	Rat	2 μ g/mL	BD Pharmingen
CD34	Stem cells	PE	IgG2a κ	RAM34	Rat	2 μ g/mL	BD Pharmingen
CD115	Phagocytic precursor	PE	IgG1 κ	T38-320	Rat	5 μ g/mL	BD Pharmingen
CD14	Monocytes/macrophages	PE	IgG1 κ	rmC5-3	Rat	2 μ g/mL	BD Pharmingen
CD150	Lymphoid cells	PE	IgG2a κ	Q38-480	Rat	2 μ g/mL	BD Pharmingen
CD62L	BM inflamed cells	PE-Cy	IgG2a κ	MEL-14	Rat	4 μ g/mL	BD Pharmingen
CD31	BM inflamed cells	PE	IgG2a κ	MEC 13.3	Rat	2 μ g/mL	BD Pharmingen
CCR2	BM inflamed cells	PE	IgG2b	475301	Rat	2 μ g/mL	R&D systems
CX ₃ CR1	Resident cells in BM	PE	IgG2a κ	SA011F11	Mouse	5 μ g/mL	BioLegend

Notes.

a: PE: phycoerythrin; PE-Cy7: phycoerythrin-Cyanine 7

b: Bp: *Burkholderia pseudomallei*

c: poly: polyclonal antibodies

Co., Chicago, IL, USA) density gradient centrifugation (800 \times g, 30 min). Red blood cell contamination was removed by treating the cells with 0.83% NH₄Cl for 3 min, followed by rapid neutralization using 2% fetal calf serum (FCS)-PBS. BM suspensions were prepared from the liquid obtained from flushing the BM and filtered using nylon membranes (30 μ m; Millipore, Billerica, MA, USA). Hepatic cell suspensions were sequentially prepared by scraping and digesting tissue using a solution (1 mg/mL collagenase and 5 mM CaCl₂ in PBS) followed by filtering using a nylon membrane (70 μ m; Millipore), gradient centrifugation (30–70% Percoll in PBS), and harvesting of the mononuclear layers. The BILs were retrieved from the brains of the mice with melioidosis after perfusion. After homogenization, the leukocyte layers were harvested *via* centrifugation in 30% Percoll in PBS at 500 \times g for 30 min. The myelin debris was removed using a mesh cell strainer filter (40 μ m; Miltenyi Biotech., Bergisch Gladbach, Germany). After washing with RPMI (Roswell Park Memorial Institute) 1640 medium (Sigma, St. Louis, MO, USA), the cells were suspended in 1 mL of FACS (2% bovine serum albumin and 0.02% sodium azide in calcium and magnesium-free PBS) and transferred to 1 mL of Ficoll-Paque Plus solution (GE Healthcare Life Science Co.). After centrifugation at 1,400 \times g for 25 min, the layer containing the BILs was collected, washed with FACS, and maintained in a 2% FCS-PBS solution. Peripheral blood (*ca.* 100 μ L) was collected from the tail vein and rapidly diluted with 100 μ L PBS. The diluted blood was subjected to density gradient centrifugation with an equal volume of Ficoll-Paque (400 \times g, 20 min). After centrifugation, the mononuclear cell

layers were collected, neutralized with PBS and maintained in a 2% FCS-PBS solution.

Flow cytometry analysis

Single-cell preparations in 2% FCS-PBS were incubated with specific monoclonal PE (phycoerythrin)- or PE-Cy (cyanine) 7-conjugated anti-mouse antibodies for 30 min on ice in the dark according to the manufacturer's protocol. The clones, isotype controls, origins and concentrations of the antibodies are shown in Table 1. After incubation, the numbers of stained cells were estimated by flow cytometry using appropriate gating (Cell Lab Quanta SC; Beckman Coulter, Inc., Brea, CA, USA). To determine the proportions (%) of each cellular subpopulation (10⁶ cells in the BM, splenic and hepatic subpopulations, 10⁵ cells in the blood and 4 \times 10⁴ in the BILs), the flow cytometry data were analyzed using CXP software (Beckman Coulter, Inc.).

Bacterial loads in organs

The melioidosis mice were sacrificed at the indicated times after infection. The solid organs (spleen, 0.02 g; liver, 0.5 g; lung, 0.01 g; and brain, 0.4 g) were excised and homogenized in 500 μ L of 2% FCS-PBS. The melioidosis mice were assigned into bacteremic and non-bacteremic groups according to blood cultures from tail veins. The BM cells were aseptically flushed from the femur using 1 mL of 2% FCS-PBS. The total numbers of bacteria in the BM (CFU/mL) or the organs (g/mL) were determined using serial dilutions and the plate count method. The limits of detection were 20, 50, 50 and 3 CFU/g for the liver, spleen, lung and brain and 10 CFU/mL for BM.

Adoptive transfer

Donor cells were prepared from BM Ly6C cells harvested from wild-type or KO mice. On d 14 post-infection, the mice were confirmed to have bacteremia using blood cultures from the tail vein. A single-cell suspension of BM Ly6C⁺ cells was isolated using an EasySep Mouse Positive Selection Kit (STEMCELL Tech. Inc., Vancouver, Canada). Prior to adoptive transfer, the donor cells were confirmed to contain 18–22% Ly6C⁺GFP⁺ cells. The donor cells were treated with 400 µg/mL kanamycin in 2% FCS-PBS to remove extracellular bacteria. After treatment, the numbers of intracellular *B. pseudomallei* were determined. Under this condition, approximately 10⁵ CFU of *B. pseudomallei* GFP were present in 1.4 × 10⁶ *sell*^{-/-}*selp*^{+/+}, 4.6 × 10⁵ *sell*^{+/+}*selp*^{-/-} and 3.3 × 10⁵ *sell*^{+/+}*selp*^{+/+} Ly6C cells. If the bacterial numbers were >±10 % of 10⁵ CFU on the next day, the data for adoptive transfer were omitted.

Ly6C cells harboring 10⁵ CFU of *B. pseudomallei* were used as donor cells. As controls, the same number of wild-type Ly6C cells were admixed with free *B. pseudomallei* (10⁵ CFU) and used for adoptive transfer. The recipient mice (uninfected C57BL/6 female mice, 8–10 weeks old) were adoptively transferred *via* intravenous injection. After 4 d, the bacterial loads in the brain were determined by serial dilution and the plate count method. The percentage (%) of Ly6C⁺GFP⁺ cells in the BILs (4 × 10⁴ cells) was determined using flow cytometry analysis (see above).

Antibody treatment of donor cells

The BM Ly6C cells were respectively purified from BALB/c, C57BL/6 and KO mice with bacteremic melioidosis in accordance with the above protocols. The numbers (10⁵ CFU) of intracellular *B. pseudomallei* in Ly6C cells were confirmed by flow cytometry analysis and the plate count method (see above and reference 20). The neutralizing antibody used was sodium azide-free rat anti-CD62L monoclonal antibody (clone number, MEL-14; isotype, IgG2a; Abcam Co., Cambridge, UK). Control IgGs were prepared from rabbit total IgGs.³¹ Following repeated pre-absorptions using C57BL/6 and BALB/c

BM (10⁷) cells, the IgG fractions were purified using a protein A purification kit (GenScript USA Inc., Piscataway, NJ, USA). For adoptive transfer, the donor cells were pre-incubated with antibody (5 µg/10⁵ cells) for 15 min on ice. Donor cells pre-incubated with bovine serum albumin (BSA; 5 µg/10⁵ cells) for 15 min on ice were used as another protein control. The protocols for adoptive transfer were followed as above.

Statistical analysis

All data regarding the proportion of each cellular subpopulation and bacterial loads in organs or BM are expressed as the means ± SD from independent mice (n = 6) in 2 experiments. Differences between the 2 experimental groups were analyzed using a Mann-Whitney U test. Comparisons between multiple groups were analyzed using ANOVA and the Tukey HSD test. Significance was set at *p* < 0.05.

Results

Persistence of *B. pseudomallei* in multiple organs

Neurologic melioidosis has been established in BALB/c mice *via* intravenous injection (50 CFU of *B. pseudomallei* GFP).²⁰ In this study, we characterized the persistence of *B. pseudomallei* GFP in a variety of phagocytes, such as CD11b⁺ leukocytes, Ly6C⁺ monocytes, Ly6G⁺ neutrophils and F4/80⁺ macrophages, in the organs (BM, spleen and liver), BILs and peripheral blood cells of melioidosis mice. After 14 d of infection, the CD11b⁺GFP⁺ and Ly6C⁺GFP⁺ cells among the BM, splenic or hepatic cells as well as the CD11b⁺GFP⁺ and F4/80⁺GFP⁺ cells in the BILs or blood cells were the predominant populations (Table 2).

After infection of *B. pseudomallei*, a total of 10 BALB/c mice were sacrificed and histologically examined at d 14 post-infection. Sixty percent (6/10) of the mice exhibited meningeal neutrophil infiltration (Fig. 2A) and/or multiple abscesses in the brain (Fig. 2B). Both CD11b (Fig. 2C) and Ly6C cells (Fig. 2D) infiltrated the meninges. Many

Table 2. Distribution of *B. pseudomallei* GFP in cellular subpopulations in multiple organs on d 14 post-infection.

	Distribution of GFP-positive cells in cellular subpopulations (%) ^a			
	CD11b ⁺ GFP ⁺	Ly6C ⁺ GFP ⁺	Ly6G ⁺ GFP ⁺	F4/80 ⁺ GFP ⁺
Bone marrow cells	21.7 ± 1.8	22.0 ± 1.4	9.7 ± 0.5	8.5 ± 5.2
Splenic mononuclear cells	20.3 ± 1.8	16.3 ± 0.9	8.1 ± 2.3	4.5 ± 0.6
Hepatic mononuclear cells	43.6 ± 2.1	43.4 ± 5.5	12.4 ± 2.7	36.7 ± 0.9
Brain-infiltrating leukocytes	53.4 ± 5.4	7.8 ± 2.9	2.7 ± 0.8	38.4 ± 2.9
Blood cells	15.5 ± 0.8	10.9 ± 1.5	1.5 ± 0.6	14.0 ± 1.3

Notes. a, The data from d 0 post-infection are not shown because <0.5% of the GFP signals were detected in all of the subpopulations. The proportions (%) of each cellular subpopulation (10⁶ cells in the BM, splenic and hepatic subpopulation, 10⁵ cells in blood and 4 × 10⁴ in BILs) are shown.

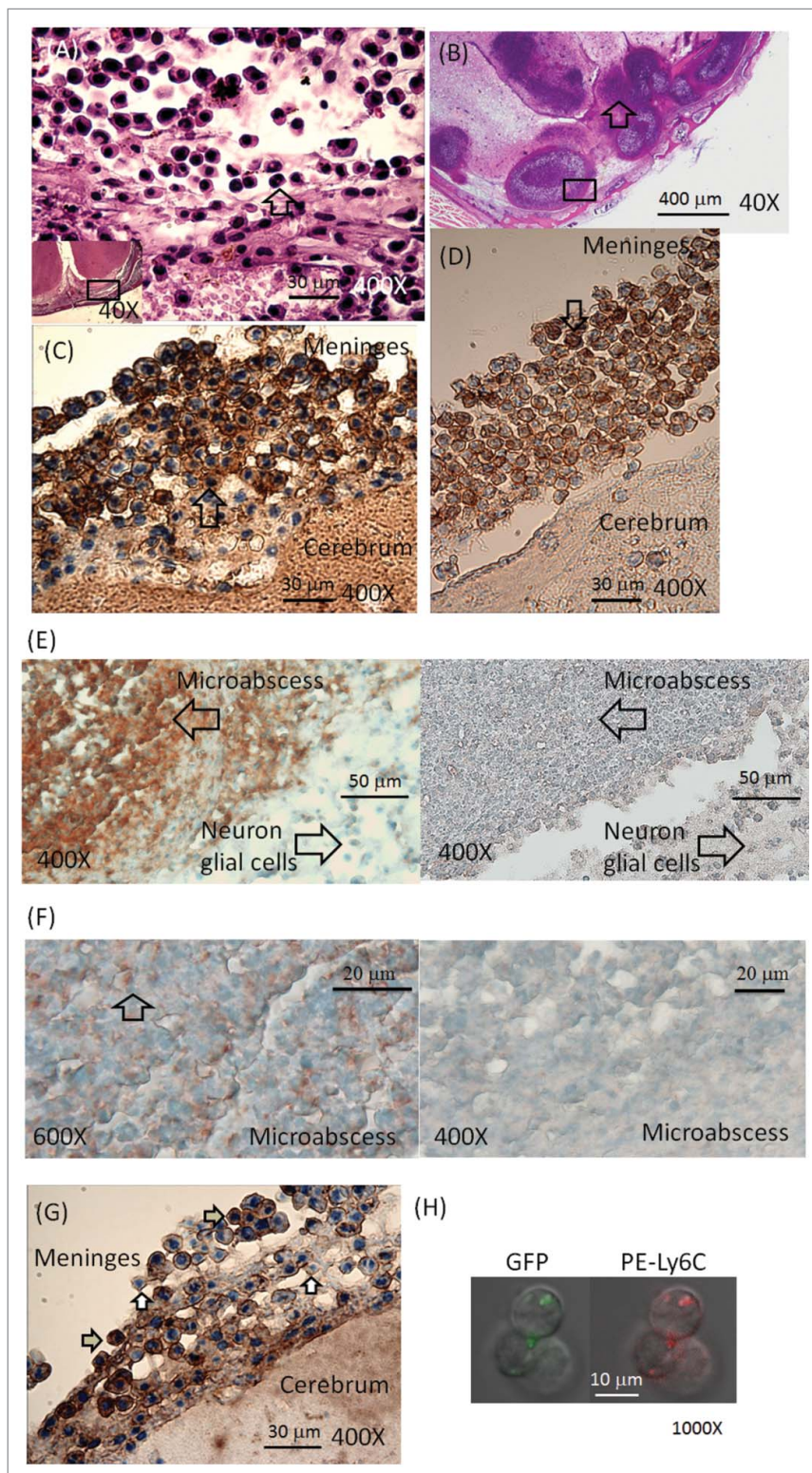


Figure 2. Histological examination. Melioidosis was induced in BALB/c mice by intravenous infection. On d 14 post-infection, meningeal neutrophil (indicated by arrows) infiltration (A, 400X; magnification of the lower left square, 40X) and cerebral microabscesses (B, 40X, indicated by arrows) were assessed using H&E staining. Anti-CD11b (C, 400X; indicated by arrows) and anti-Ly6C (D, 400X; indicated by arrows) antibodies were used to label cells in the meninges (representative localization in the square of Fig. 1A), and anti-Ly6G (E, 400X; fragments indicated by arrows on left; stained with isotype control on right) and anti-F4/80 (F, fragments indicated by arrows on left [600X]; stained with isotype control on right [400X]) antibodies were used to label their respective antigens in the fragments of the cerebral abscesses (representative localization in the square of Fig. 1B). A number of intracellular *B. pseudomallei*-specific antigens (positive indicated by gray arrows; negative indicated by white arrows) in brain-infiltrating leukocytes (BILs) are shown (G, 400X). The GFP and Ly6C signals observed in BILs *via* confocal microscopy are shown (H, 1,000X).

Ly6G (Fig. 2E) and F4/80 (Fig. 2F) antigens were present in the fragments of the cerebral abscesses. CD3e lymphocytes or CD19 B cells were rarely observed in the inflamed sites (data not shown). Numerous intracellular *B. pseudomallei*-specific antigens were observed in the meningeal-infiltrating cells (Fig. 2G). Confocal microscopy revealed intracellular *B. pseudomallei* GFP present in the BILs (Fig. 2H, representative of Ly6C cells).

Kinetic study of circulating and resident phagocytes in BILs

The BILs originate from the blood circulating CD16/32⁺CD45^{hi} phagocytes and brain resident CD16/

32⁺CD45^{lo} microglia.³² The kinetics of both subpopulations showed that the circulating CD16/32⁺CD45^{hi} cells increased from $0.8 \pm 0.1\%$ (d 0) to $5.5 \pm 0.4\%$ (d 4). No increase was observed from d 4 to d 7; however, those circulating cells increased again after 7 d of infection. For the resident CD16/32⁺CD45^{lo} microglia, the number was not significantly increased by d 4 post-infection but reached a plateau after 7 d of infection (Fig. 3A).

Less than 0.2% each of the CD16/32⁺CD45^{hi} and CD16/32⁺CD45^{lo} subpopulations in the BILs were *B. pseudomallei* GFP-positive by d 2 post-infection, whereas $7.9 \pm 1.4\%$ of the CD16/32⁺CD45^{hi} cells and $22.5 \pm 5.4\%$ of the CD16/32⁺CD45^{lo} cells were positive at d 4 post-infection. After this time point, the GFP-positive cells

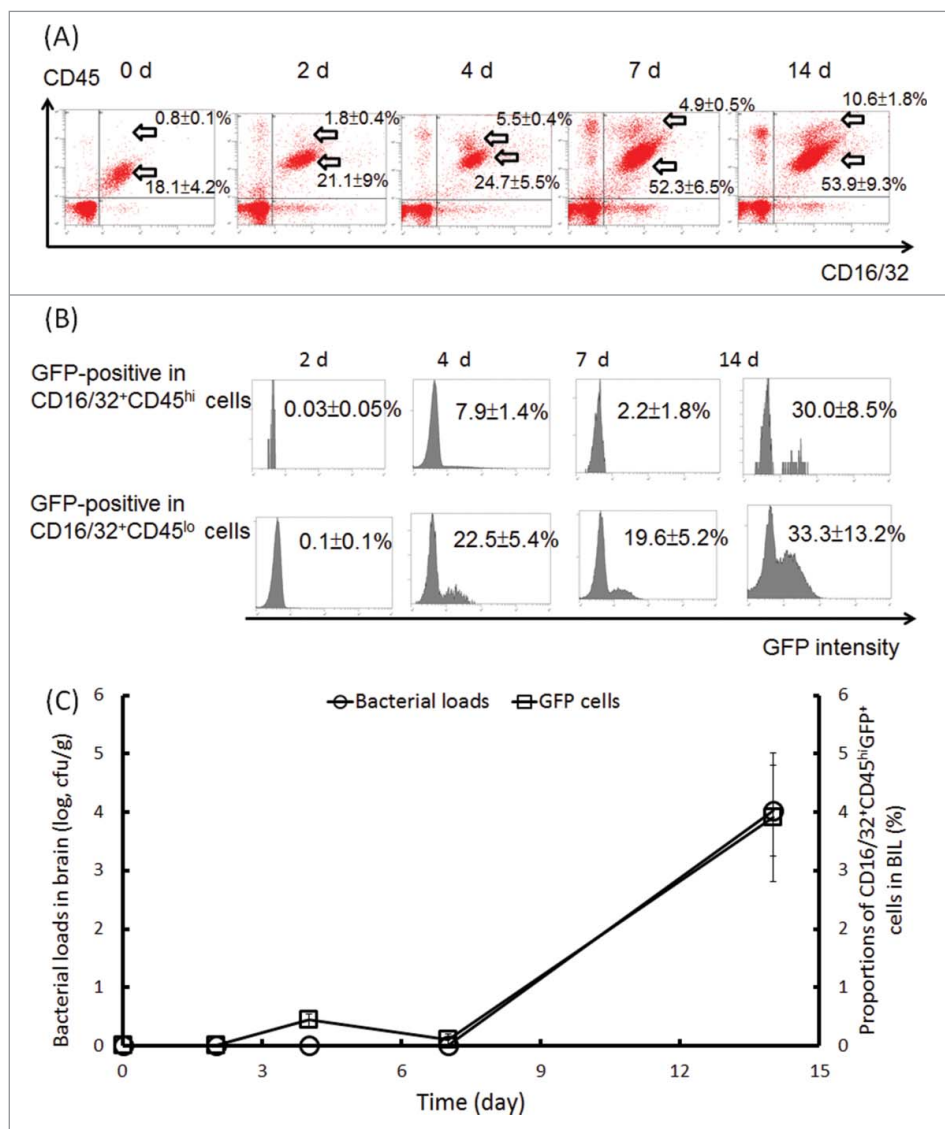


Figure 3. Expansion of the CD16/32⁺CD45^{hi} and CD16/32⁺CD45^{lo} subpopulations and persistence of *B. pseudomallei* in cells and brain tissues. BILs were isolated from BALB/c melioidosis mice at the indicated time points. The expansion of the CD16/32⁺CD45^{hi} and CD16/32⁺CD45^{lo} subpopulations (A) and the changes in the *B. pseudomallei* GFP signals in both subpopulations (B) are shown. The numbers of *B. pseudomallei* in the brain homogenates (CFU/g) at the indicated times were determined using the plate count method. The CD16/32⁺CD45^{hi}GFP⁺ cells were estimated using flow cytometry analysis (C).

were restricted to $2.2 \pm 1.8\%$ in the $CD16/32^+CD45^{hi}$ and $19.6 \pm 5.2\%$ in the $CD16/32^+CD45^{lo}$ BIL subpopulations. At d 14 post-infection, the *B. pseudomallei*-loaded BILs had again expanded ($30.0 \pm 8.5\%$ GFP-positive cells in the $CD16/32^+CD45^{hi}$ subpopulation; $33.3 \pm 13.2\%$ GFP-positive cells in the $CD16/32^+CD45^{lo}$ subpopulation) (Fig. 3B). Based on plate counts of *B. pseudomallei* in brain homogenates, we found that the cultivated *B. pseudomallei* were not found by d 7 post-infection but that they reached $>10^4$ CFU/g on d 14 post-infection. Accordingly, the proportion of the $CD16/32^+CD45^{hi}GFP^+$ cells in the BILs was increased from $<0.2\%$ on d 7 to $3.9 \pm 1.1\%$ on d 14 post-infection (Fig. 3C).

Incidence of neurologic melioidosis in resistant C57BL/6 mice

As is known, C57BL/6 mice are more resistant to *B. pseudomallei* than BALB/c mice.¹² The survival rates of the C57BL/6 melioidosis mice were 100% (20/20) at 5×10^4 CFU, 80% (16/20) at 5×10^5 CFU and 35% (7/20) at 5×10^6 CFU of infective doses on d 14 post-infection (Fig. 4A). At 5×10^5 CFU of the infective dose, the *B. pseudomallei* loads in the organs varied. Once bacteremic melioidosis was established, all of the tested organs except the brains reproducibly presented bacterial colonization (Fig. 4B). As we assumed, through the blood circulation, the *B. pseudomallei*-loaded cells crossed the BBB to induce neurologic melioidosis. In the resistant C57BL/6 mice with bacteremic melioidosis, the circulating $CD16/32^+CD45^{hi}GFP^+$ cells did not increase by d 14 post-infection, even though the resident $CD16/32^+CD45^{lo}GFP^+$ cells had expanded to $2.8 \pm 0.9\%$ at this point (Fig. 4C). The changes of proportions of both $CD16/32^+CD45^{hi}$ and $CD16/32^+CD45^{lo}$ subpopulations in BILs were shown in Table 3. On d 14 post-infection, there were no cultivated *B. pseudomallei* from the C57BL/6 brains with melioidosis (Fig. 4B). Only 10% meningeal neutrophil infiltration was estimated for the C57BL/6 mice with melioidosis (Fig. 4A). Given that the $CD16/32^+CD45^{hi}$ cells were derived from Ly6C monocytes in the BM, the question of whether *B. pseudomallei* persisted in the C57BL/6 BM cells was raised.

Maturation and expansion of cellular subpopulations in BM

In a previous study, we demonstrated that all BALB/c mice can be induced to develop bacteremic melioidosis after 4 d of intravenous infection. The $CD11b^+Ly6C^+$ monocytes in the BM accounted for 18% of all BM cells on d 0, but this percentage increased to 71.1% by d 10 post-infection. The colonization of *B. pseudomallei* in BALB/c BM can reach

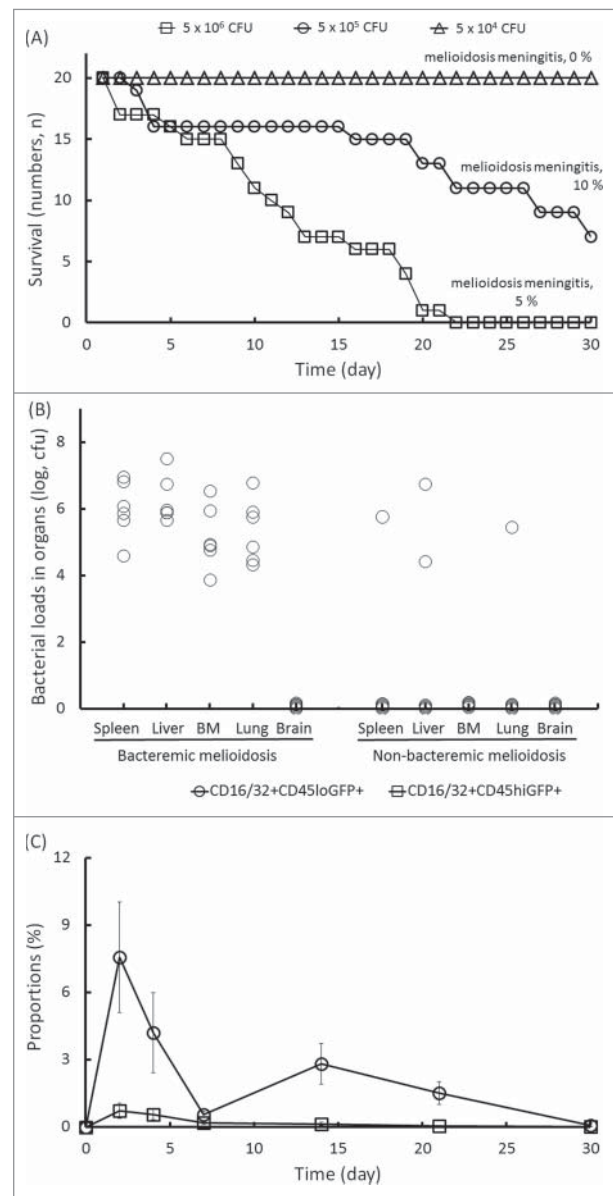


Figure 4. Manifestation of melioidosis in C57BL/6 mice. C57BL/6 mice were intravenously infected with 5×10^4 , 5×10^5 and 5×10^6 CFU of *B. pseudomallei* GFP. During a 30-d infection, the daily survival rates were recorded, and the percentages of mice with neurologic melioidosis at the end of the experiment were confirmed by histological brain examination (A). In the infective doses of 5×10^5 CFU of *B. pseudomallei* GFP, the bacterial loads in the organs ($n = 6$; spleen, liver, lung, BM and brain) for melioidosis with bacteremia or non-bacteremia on d 14 post-infection are shown (B). The changes in the numbers of circulating $CD16/32^+CD45^{hi}GFP^+$ cells and resident $CD16/32^+CD45^{lo}GFP^+$ cells in the brain-infiltrating leukocytes during melioidosis are shown (C).

10^4 CFU/mL.²⁰ In the present study, during bacteremic melioidosis for C57BL/6 mice, the proportions of each subpopulation in BM fluctuated (Table 3). We found that the $CD11b^+CD34^+GFP^+$ haematopoietic stem cells and the $CD11b^+CD115^+GFP^+$ phagocytic precursors (Fig. 5A), the $CD11b^+CD14^+GFP^+$ LPS-responding activated

Table 3. Distribution of the subpopulations in BILs or BM for the C57BL/6 mice with melioidosis.

	Proportions (%) of subpopulations at infection of						
	0 d	2 d	4 d	7 d	14 d	21 d	30 d
in BIL ^a							
CD16/32 ⁺ CD45 ^{hi} (circulating phagocytes)	<0.1	1.55 ± 0.3	1.05 ± 0.2	0.2 ± 0.1	0.3 ± 0.1	0.2 ± 0.1	<0.1
CD16/32 ⁺ CD45 ^{lo} (resident microglia)	<0.2	10.4 ± 2.5	8.8 ± 0.9	4.0 ± 0.4	7.4 ± 0.8	2.9 ± 0.3	0.6 ± 0.4
in BM ^b							
CD11b ⁺ CD34 ⁺ (stem cells)	1.8 ± 0.3	7.3 ± 3.2	7.9 ± 6.1	2.9 ± 1.2	9.7 ± 1.2	4.6 ± 4.5	11.2 ± 7.5
CD11b ⁺ CD115 ⁺ (phagocytic progenitors)	12.0 ± 1.4	19.7 ± 6.9	7.9 ± 4.9	7.9 ± 5.3	8.0 ± 5.5	4.0 ± 4.0	7.1 ± 1.5
CD11b ⁺ Ly6C ⁺ (monocytes)	58.6 ± 9.7	82.0 ± 9.2	80.3 ± 6.8	85.6 ± 0.5	84.4 ± 0.9	88.7 ± 12.4	69.1 ± 1.4
CD11b ⁺ Ly6G ⁺ (neutrophils)	33.3 ± 0.8	36.1 ± 1.6	65.4 ± 20.0	73.6 ± 16.0	55.6 ± 25.0	53.9 ± 23.0	46.6 ± 19.0
CD11b ⁺ F4/80 ⁺ (macrophages)	9.4 ± 0.9	34.1 ± 23.0	21.9 ± 3.3	13.0 ± 1.8	11.4 ± 7.0	6.4 ± 3.2	10.7 ± 0.2
CD11b ⁺ CD14 ⁺ (activated macrophages)	0.8 ± 0.3	25.2 ± 3.8	16.4 ± 7.4	6.7 ± 5.0	10.4 ± 2.6	3.5 ± 3.3	2.0 ± 0.4
CD11b ⁺ CD150 ⁺ (lymphoid cells)	1.3 ± 0.1	6.4 ± 2.9	4.9 ± 3.6	1.5 ± 0.1	13.1 ± 4.0	4.2 ± 4.0	11.2 ± 7.5
Ly6C ⁺ CD62L ⁺ (inflamed cells)	12.6 ± 3.4	37.9 ± 14.2	55.0 ± 13.7	34.0 ± 29.0	22.3 ± 19.2	71.6 ± 7.8	26.1 ± 5.2
Ly6C ⁺ CCR2 ⁺ (inflamed cells)	6.6 ± 2.0	6.8 ± 2.3	11.9 ± 5.4	44.5 ± 36.7	14.5 ± 10.9	9.3 ± 6.5	11.2 ± 7.5
Ly6C ⁺ CD31 ⁺ (inflamed cells)	6.5 ± 1.4	58.2 ± 17.2	55.3 ± 14.0	26.6 ± 8.8	15.1 ± 10.8	17.7 ± 5.0	23.6 ± 9.9
Ly6C ⁺ CX ₃ CR1 (resident cells)	7.4 ± 3.7	51.8 ± 9.9	55.3 ± 38.3	56.4 ± 43.2	44.1 ± 22.0	16.1 ± 1.6	11.2 ± 7.5

Notes.a, brain-infiltrating leukocytes (4×10^4 cells)b, bone marrow cells (10^6 cells)

macrophages, the CD11b⁺Ly6C⁺GFP⁺ monocytes, the CD11b⁺Ly6G⁺GFP⁺ neutrophils and the CD11b⁺F4/80⁺GFP⁺ macrophages (Fig. 5B), as well as the CD11b⁺CD150⁺GFP⁺ lymphoid cells (T, B and natural killer cells) (Fig. 5C) were increased on d 2 and d 14 post-infection. The major reservoirs of *B. pseudomallei* were distributed in CD11b⁺Ly6C⁺ and CD11b⁺Ly6G⁺ BM cells on d 14 post-infection.

The *B. pseudomallei*-loaded BM cells provided a risk of systemic dissemination *via* blood circulation. Thus, we examined surface markers (the chemokine receptors CCR2 and CX₃CR1, L-selectin [CD62L] and the platelet endothelial cell adhesion molecule CD31) that indicated that the inflammatory cells in the BM were ready for migration into the blood. The proportions of Ly6C⁺CCR2⁺GFP⁺, Ly6C⁺CX₃CR1⁺GFP⁺, Ly6C⁺CD62L⁺GFP⁺ and Ly6C⁺CD31⁺GFP⁺ cells fluctuated during melioidosis. Although the numbers of Ly6C⁺CX₃CR1⁺GFP⁺, Ly6C⁺CD62L⁺GFP⁺ and Ly6C⁺CD31⁺GFP⁺ cells had increased by d 2 post-infection, the Ly6C⁺CX₃CR1⁺GFP⁺ cells on d 14 and Ly6C⁺CD62L⁺GFP⁺ cells on d 21 were the predominant *B. pseudomallei*-loaded subpopulations (Fig. 6A).

The growth of *B. pseudomallei* in C57BL/6 BM was restricted at the initial infection. There were few viable *B. pseudomallei* (<2000 CFU/mL) in the BM by d 14 post-infection; the bacterial loads in the BM reached $>4.5 \times 10^5$ CFU/mL after 14 d of infection in bacteremic mice (Fig. 6B). Ly6C⁺CD62L⁺ cells represent mature inflamed cells that are ready to migrate from BM, whereas Ly6C⁺CX₃CR1⁺ cells represent the resident monocytes in the BM.²⁵ In a previous study, we demonstrated that the incidence of neurologic melioidosis was associated with the appearance of L-selectin-expressing

BALB/c CD11b leukocytes infected with *B. pseudomallei*. Thus, according to the Trojan horse hypothesis, the appearance of Ly6C⁺CD62L⁺GFP⁺ inflamed cells after 14 d of infection indicates a risk for the induction of neurologic melioidosis.

Induction of melioidosis meningitis via Ly6C cell migration

To demonstrate that the *B. pseudomallei*-loaded BM Ly6C⁺CD62L⁺ cells contributed to the development of neurologic melioidosis, the C57BL/6 BM Ly6C donor cells were isolated from the *sell*^{-/-}*selp*^{+/+}, *sell*^{+/+}*selp*^{-/-} and *sell*^{+/+}*selp*^{+/+} melioidosis mice and adjusted to an equal number of *B. pseudomallei* GFP for each group (10^5 CFU; *ca.* 1.4 ± 6 of *sell*^{-/-}*selp*^{+/+} Ly6C cells, 4.6 ± 10^5 of *sell*^{+/+}*selp*^{-/-} Ly6C cells, 3.3 ± 10^5 of *sell*^{+/+}*selp*^{+/+} Ly6C cells; see Materials and Methods). After adoptive transfer of the *B. pseudomallei*-loaded *sell*^{+/+}*selp*^{+/+} or *sell*^{+/+}*selp*^{-/-} Ly6C cells, the bacterial loads in the wild-type recipient brains were increased to $>5 \times 10^4$ CFU/g. In contrast, only <110 CFU/g of bacteria were present in the recipient brain after adoptive transfer of the *B. pseudomallei*-loaded *sell*^{-/-}*selp*^{+/+} Ly6C cells (Fig. 7A). To exclude the possibility that *B. pseudomallei* directly invaded the brain tissue, 10^5 CFU of free bacteria mixed with wild-type non-infected Ly6C cells was immediately injected into the mice, and bacterial colonization due to this control treatment was not observed in the recipient brains (Fig. 7A). We observed that the proportions of Ly6C⁺GFP⁺ BILs in the recipient mice were increased to $1.6 \pm 0.6\%$ after adoptive transfer of the *B. pseudomallei*-loaded *sell*^{+/+}*selp*^{-/-} Ly6C cells and $1.7 \pm 0.7\%$ for *B. pseudomallei*-loaded *sell*^{+/+}*selp*^{+/+} Ly6C cells;

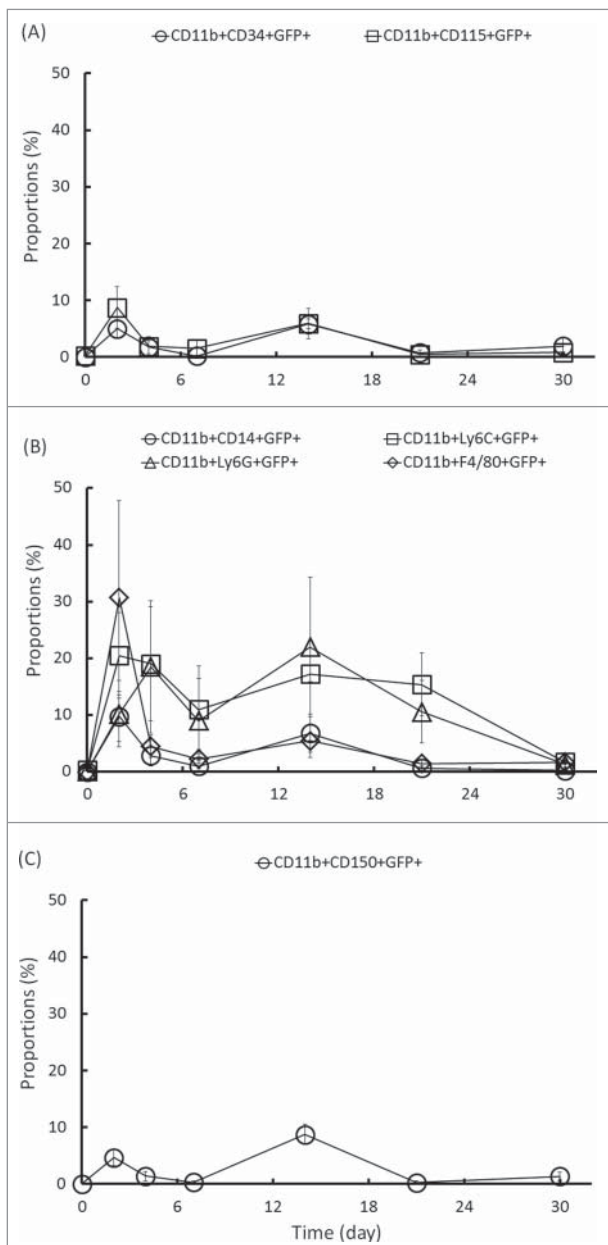


Figure 5. Changes in the number of GFP-positive cells in the BM CD11b subpopulation. A single-cell suspension was prepared from the BM of C57BL/6 mice during melioidosis. The changes in the numbers of phagocytic precursor CD11b⁺CD34⁺GFP⁺ and CD11b⁺CD115⁺GFP⁺ cells (A), phagocyte CD11b⁺CD14⁺GFP⁺, CD11b⁺Ly6C⁺GFP⁺, CD11b⁺Ly6G⁺GFP⁺ and CD11b⁺F4/80⁺GFP⁺ cells (B), and lymphoid lineage CD11b⁺CD150⁺GFP⁺ cells (C) were analyzed.

however, only $0.25 \pm 0.04\%$ of Ly6C⁺GFP⁺ BILs were present in recipient mice after adoptive transfer of *B. pseudomallei*-loaded *sell*^{-/-}*sefp*^{+/+} Ly6C cells (Fig. 7B).

To determine whether CD62L is one of the key factors in inducing neurologic melioidosis, the donor cells isolated from both the C57BL/6 and the BALB/c mouse models were pretreated with a neutralizing anti-CD62L antibody. After adoptive transfer of anti-CD62 antibody-

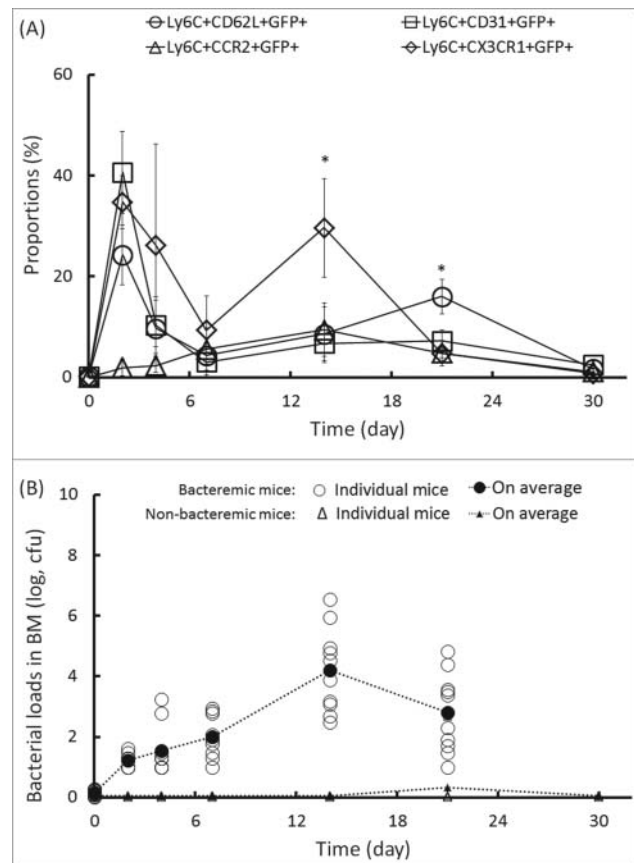


Figure 6. Expansion of GFP-positive cells in the BM Ly6C subpopulation and persistence of *B. pseudomallei* in the bone marrow. At the indicated times after infection, the changes in the numbers of Ly6C⁺CD62L⁺GFP⁺, Ly6C⁺CD31⁺GFP⁺, Ly6C⁺CCR2⁺GFP⁺ and Ly6C⁺CX₃CR1⁺GFP⁺ cells (A) and cultivated *B. pseudomallei* (B) in the BM of bacteremic (circles) and non-bacteremic (triangles) mice were determined. No bacteremic mouse was found on d 30 post-infection. The (*) symbol indicates $p < 0.05$ (ANOVA and Tukey HSD test).

treated Ly6C cells infected with *B. pseudomallei*, bacterial colonization of recipient BALB/c and C57BL/6 brains was significantly depleted compared to that in the control mouse groups in which the donor cells were pretreated with control IgG or BSA (Fig. 7C). We suggest that the BM Ly6C⁺CD62L⁺ monocytes harboring *B. pseudomallei* migrated to the brain *via* the circulation and subsequently triggered the incidence of neurologic melioidosis in both mouse models.

Discussion

Previously, we found that *B. pseudomallei*-loaded selectin-expressing splenic CD11b cells elicit bacterial colonization of BALB/c brains following adoptively transfer.²⁰ In the present study, we further demonstrated the existence of a selectin (CD62L)-dependent leukocyte-mediated Trojan horse mechanism during mouse melioidosis.

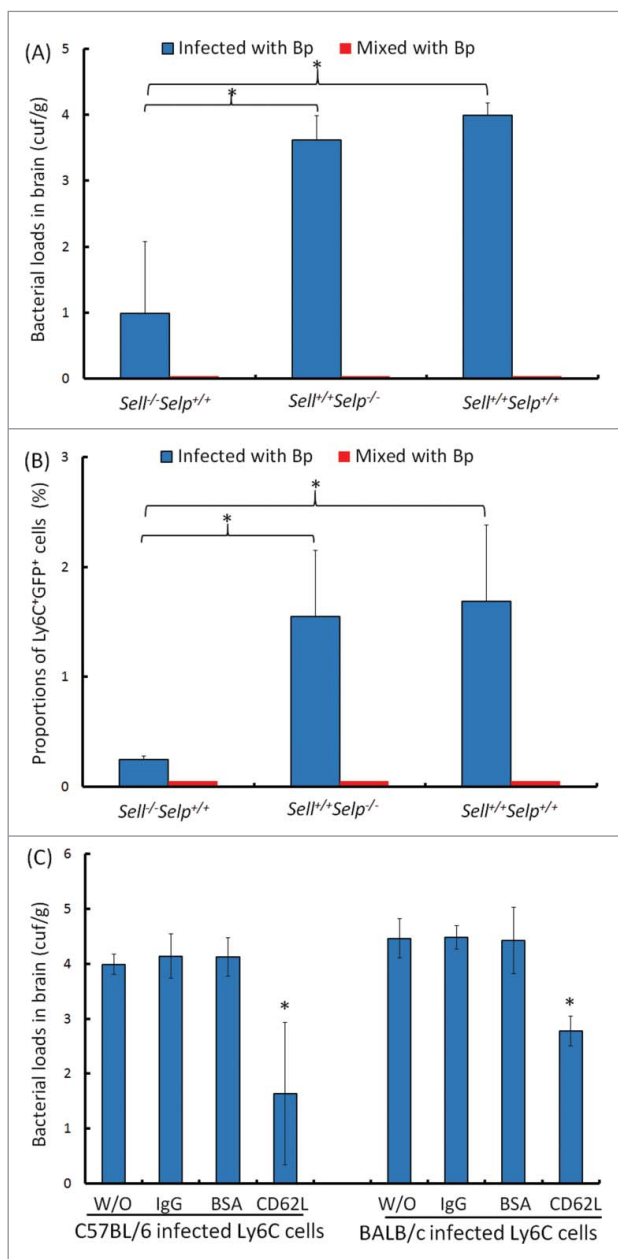


Figure 7. Adoptive transfer. The C57BL/6 BM *sell^{+/+}selp^{+/+}*, *sell^{-/-}selp^{+/+}* and *sell^{+/+}selp^{-/-}*-Ly6C cells or BALB/c BM harboring 10^5 CFU of *B. pseudomallei* were used as donors (blue). As controls, the Ly6C cells were immediately mixed with 10^5 CFU of free *B. pseudomallei* (red). After adoptive transfer of *sell^{+/+}selp^{+/+}*, *sell^{-/-}selp^{+/+}* and *sell^{+/+}selp^{-/-}*-cells, the bacterial colonization of brains (A) and proportions of Ly6C⁺GFP⁺ cells (B) were determined for C57BL/6 recipients. For antibody blocking, the *B. pseudomallei*-loaded C57BL/6 or BALB/c BM Ly6C cells were pretreated with anti-CD62L antibody (CD62L), rabbit control IgGs (IgG) or bovine serum albumin (BSA) or were without treatment (W/O). After adoptive transfer, the bacterial colonization of brains in C57BL/6 and BALB/c recipients was respectively shown. The (*) symbol indicates $p < 0.05$ between lined groups (Mann-Whitney U test for Fig. 7A and 7B) or multiple groups (ANOVA and Tukey HSD test for Fig. 7C).

Firstly, the bacterial colonization of the brain was enhanced in recipient C57BL/6 mice *via* adoptive transfer of *B. pseudomallei*-loaded *sell^{+/+}* Ly6C cells compared to the results of adoptive transfer of free *B. pseudomallei* or infected *sell^{-/-}* Ly6C cells. Secondly, anti-CD62L antibody interrupted *B. pseudomallei*-loaded C57BL/6 and BALB/c cells' invasion of the CNS.

The leukocyte-mediated Trojan horse mechanism is summarized in Fig. 8. During melioidosis, microabscesses develop secondary to primary foci *via* hematogenous routes, and *B. pseudomallei* steadily persists in CD11b⁺Ly6C⁺ monocytes, CD11b⁺Ly6G⁺ neutrophils and CD11b⁺F4/80⁺ macrophages in the inflamed liver and spleen during early infection (by d 4 post-infection) (Fig. 8A, step 1).^{20,33} Intracellular survival is an important step in the bacterial dissemination *via* the hematogenous route, as mice infected with a *B. pseudomallei* *bas* mutant that had lost the ability to survive intracellularly experienced prolonged survival during melioidosis.^{34,35} In some cases, bacteremia temporally disappears after 4 d of infection.²⁰ However, both the liver and the spleen become *B. pseudomallei* reservoirs.^{20,33} *B. pseudomallei*-loaded splenic CD11b cells were demonstrated to improve *B. pseudomallei* invasion of the brain (Fig. 8A, step 2)²⁰ although the mechanisms of *B. pseudomallei* reloading into the blood *via* infected monocyte-derived kupffer cells (CD11b⁺F4/80⁺) or splenic follicular DCs (CD11b⁺CD11c⁺) remain unknown. Once bacteremia recurs or persists (Fig. 8A, step 3), *B. pseudomallei* invades CD11b⁺CD34⁺ and CD11b⁺CD115⁺ phagocytic progenitors (Fig. 5A), differentiated CD11b⁺Ly6C⁺ monocytes, CD11b⁺Ly6G⁺ neutrophils, CD11b⁺F4/80⁺ macrophages and activated CD11b⁺CD14⁺ LPS-responding macrophages (Fig. 5B), as well as lymphoid-lineage CD11b⁺CD150⁺ cells (Fig. 5C) in the BM (Fig. 8A, step 4). The inflamed CD11b⁺CCR2⁺, CD11b⁺CD62L⁺ and CD11b⁺CD31⁺ BM cells infected with *B. pseudomallei* are matured and ready for emigration (Fig. 6A; Fig. 8A, step 5). During late infection (on d 21 post-infection), the inflamed Ly6C⁺CD62L⁺GFP⁺ cells become a predominant *B. pseudomallei*-loaded subpopulation (Fig. 6A), and consequently, the circulating monocyte-derived Ly6C and F4/80 cells harboring *B. pseudomallei* are expanded (Table 2; Fig. 8A, step 6). Acting as a Trojan horse, the infected Ly6C⁺CD62L⁺ cells cross the cerebral endothelium *via* selectin-mediated leukocyte migration, resulting in expansion of the circulating CD16/32⁺CD45^{hi} phagocytes in the BILs (Fig. 3, Fig. 4C; Fig. 8A, step 7) and, eventually, *B. pseudomallei* colonization of the brain (Fig. 2; Fig. 8A, step 8).

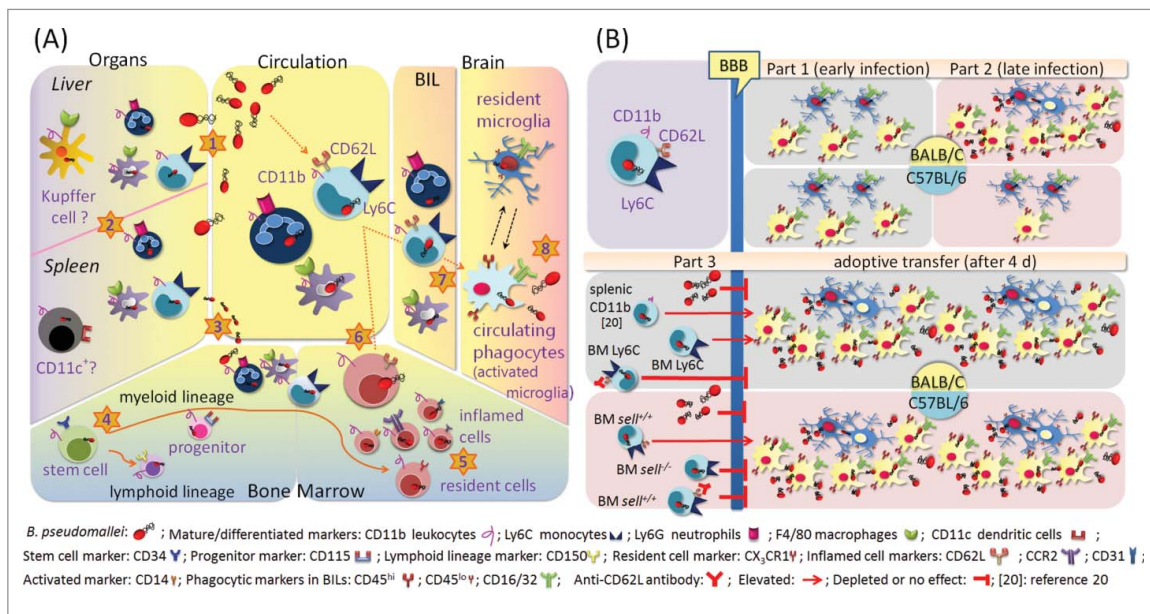


Figure 8. Summary of Trojan horse mechanism (A). During melioidosis, microabscesses develop secondary to primary foci via hematogenous routes (step 1), and *B. pseudomallei* steadily persists in CD11b⁺Ly6C⁺ monocytes, CD11b⁺Ly6G⁺ neutrophils and CD11b⁺F4/80⁺ macrophages in the liver and spleen (step 2). After 4 d of infection, the bacteremia could disappear, but the liver and spleen become *B. pseudomallei* reservoirs. Once bacteremia recurs or persists (step 3), *B. pseudomallei* invades CD11b⁺CD34⁺ stem cells and CD11b⁺CD115⁺ phagocytic progenitors and differentiated CD11b⁺Ly6C⁺ monocytes, CD11b⁺Ly6G⁺ neutrophils, CD11b⁺F4/80⁺ macrophages and activated CD11b⁺CD14⁺ LPS-responding cells, as well as lymphoid-lineage CD11b⁺CD150⁺ cells in the BM (step 4). Prior to emigration, the inflamed CD11b⁺CCR2⁺, CD11b⁺CD62L⁺ and CD11b⁺CD31⁺ BM cells harboring *B. pseudomallei* mature (step 5). On d 21 post-infection, the inflamed Ly6C⁺CD62L⁺GFP⁺ cells become a predominant *B. pseudomallei*-loaded subpopulation, and the circulating monocyte-derived CD11b⁺Ly6C⁺ and CD11b⁺F4/80⁺ cells harboring *B. pseudomallei* are expanded (step 6). Acting as a Trojan horse, the infected Ly6C⁺CD62L⁺ cells cross the cerebral endothelium via selectin-mediated leukocyte migration, resulting in expansion of the circulating CD16/32⁺CD45^{hi} phagocytes in the BILs (step 7) and eventual *B. pseudomallei* colonization of the brain (step 8). Comparison of BALB/c and C57BL/6 mice with melioidosis (B). During early infection (by d 4 post-infection), the circulating CD16/32⁺CD45^{hi}GFP⁺ phagocytes rapidly infiltrate the brains of C57BL/6 and BALB/c mice; however, the growth of intracellular *B. pseudomallei* is restricted (Part 1). On d 14 post-infection (during late infection), CD16/32⁺CD45^{lo}GFP⁺ microglia are expanded in the BILs in both BALB/c and C57BL/6 mice with melioidosis. However, in BALB/c mice with melioidosis, the CD16/32⁺CD45^{hi}GFP⁺ phagocytes are rapidly expanded in the BILs, eventually resulting in the growth of *B. pseudomallei* in the brain. However, CD16/32⁺CD45^{hi}GFP⁺ phagocytes are rarely found in C57BL/6 mice, and consequently, *B. pseudomallei* has difficulty colonizing C57BL/6 brains (Part 2). After adoptive transfer of *B. pseudomallei*-loaded splenic CD11b cells (see reference 20) or BM Ly6C cells, the bacterial loads in the recipient BALB/c brains increase. In contrast, the bacterial loads in the C57BL/6 recipient brains are decreased after adoptive transfer of *sell*^{-/-} Ly6C cells compared to adoptive transfer of *sell*^{+/+} Ly6C cells. When anti-CD62 antibody-treated Ly6C cells infected with *B. pseudomallei* act as donors, bacterial colonization of recipient BALB/c and C57BL/6 brains is also depleted. Besides, bacterial colonization of both BALB/c and C57BL/6 brains is not induced by intravenous injection of free *B. pseudomallei* (Part 3).

In our models, the C57BL/6 mice were more resistant to *B. pseudomallei* infection than the BALB/c mice were.¹²⁻¹⁶ The lethal doses of *B. pseudomallei* infection are 10- to 100-fold higher for C57BL/6 mice with melioidosis,³⁶⁻³⁸ even reaching 10⁴-fold in the present study (Fig. 4A). During early infection (by d 4 post-infection), the circulating CD16/32⁺CD45^{hi}GFP⁺ phagocytes rapidly infiltrated the brains of the C57BL/6 and BALB/c mice; however, *B. pseudomallei* were not cultivated from these brains (Fig. 3, Fig 4; Fig. 8B, part 1). We believe that the growth of *B. pseudomallei* was strictly restricted during initial infection because a down-regulation of a cell division-related gene (*ftsABH*) and cytokinesis-related genes (*minD*, *minE*) in *B. pseudomallei* at the infection site in hamsters with melioidosis has been

previously demonstrated.³⁹ Moreover, *B. pseudomallei* can intracellularly replicate in the phagocytic cytoplasm after escaping the phagosome.⁴⁰

However, intracellular *B. pseudomallei* are much more easily eradicated by C57BL/6 macrophages than by BALB/c macrophages.⁴¹⁻⁴³ Previous studies reported that after exposure to IFN- γ , C57BL/6 BM-derived macrophages express higher levels of proteins (such as respiratory chain ATPase, lysosomal enzymes and cathepsins) that are involved in oxidative killing and phagosomal function compared to BALB/c BM-derived macrophages.⁴⁴ Additionally, in *in vitro* assays, C57BL/6 macrophages kill *B. pseudomallei* more efficiently than BALB/c macrophages do, particularly following IFN- γ treatment.⁴¹⁻⁴³ In the current study, we found that

approximately 60% of BALB/c mice with melioidosis developed neurologic disorders that exhibited the BILs of CD11b leukocytes, Ly6G neutrophils, Ly6C monocytes and F4/80 macrophages harboring *B. pseudomallei* in combination with the appearance of a large amount of Ly6G and F4/80 cell debris in the brain (Fig. 2; Fig. 8B, part 2). By contrast, only 10% of infected C57BL/6 mice manifested neurologic histopathology (Fig. 3A). If the Trojan horse exists, C57BL/6 phagocytic activity certainly contributes to the intracellular persistence of *B. pseudomallei* in these cells during melioidosis. Although resident CD16/32⁺CD45^{lo}GFP⁺ cells were increased during C57BL/6 melioidosis, the C57BL/6 microglia appeared to completely restrict the growth of *B. pseudomallei* at the end of the infection period (30 d) (Fig. 4C; Fig. 8B, part 2).

The brain is an immunologically privileged organ, and the BBB is composed of highly specialized endothelial cells and astrocytes.^{45,46} When circulating free *B. pseudomallei* or *B. pseudomallei*-loaded cells move into the cerebral veins, it is believed that the innate immune cells (resident microglia, perivascular macrophages and patrolling macrophages) and intact BBB structures contribute to obstructing bacterial invasion.^{45,46} During early infection, the growth of *B. pseudomallei* in brain CD16/32⁺CD45^{hi} phagocytes and resident CD16/32⁺CD45^{lo} microglia was restricted (Fig. 3B, 3C, 4C); however, the spleen, liver or BM served as a reservoir to sustainably support the growth, eventually leading to dissemination of *B. pseudomallei* across the entire body, including the brain, via circulating free bacteria or infected cells. Moreover, *B. pseudomallei* LPS potently stimulates the production of TNF- α and NO by macrophages *in vivo*.⁴⁷ Elevated serum levels of the chemokine MCP-1 and inflammatory cytokines (TNF- α , IFN- γ , IL-6 and IL-12) have also been demonstrated during murine melioidosis.²⁰ Those cytokines and chemokines generated by systemic responding cells or by the glial cells in the brain contribute to leukocyte recruitment and the disruption of BBB integrity.^{48,49} Thus, on d 14 post-infection (during late infection) in BALB/c mice with melioidosis, the CD16/32⁺CD45^{hi}GFP⁺ phagocytes were rapidly expanded after leukocyte recruitment was increased and the BBB was attacked by inflammatory cytokines and chemokines, eventually resulting in the growth of *B. pseudomallei* in the brain during late infection (Fig. 8B, part 2). Given that phagocytic activity was higher in C57BL/6 mice than in BALB/c mice, the numbers of *B. pseudomallei*-loaded phagocytes (CD16/32⁺CD45^{hi}GFP⁺) appeared to be lower among C57BL/6 BILs than among BALB/c BILs (Fig. 3, for BALB/c; Fig. 4, for C57BL/6). Consequently, *B.*

pseudomallei had difficulty colonizing the C57BL/6 mouse brains compared to the BALB/c mouse brains (Fig. 4B; Fig. 8B, part 2).

The CD16/32⁺CD45^{hi} BILs originated from BM monocytes. The high L-selectin (CD62L)-expressing monocyte subpopulation (CD11b⁺Ly6C⁺CD62L^{hi}CCR2⁺CX₃CR1^{lo}) represents classic BM monocytes that readily migrate from BM to the inflamed site, whereas the high fractalkine (CX₃CR1)-expressing subpopulation (CD11b⁺Ly6C^{lo}CD62L⁺CCR2^{lo}CX₃CR1^{hi}) migrated to the tissue in the absence of inflammation.^{25,50,51} On d 21 post-infection, the Ly6C⁺CD62L⁺GFP⁺ inflamed cells were the predominant *B. pseudomallei*-loaded subpopulation in the BM. At this time, blood CD11b⁺Ly6C⁺GFP⁺ monocytes also became a predominant population. After adoptive transfer, we demonstrated that neurologic melioidosis was induced by both *B. pseudomallei*-loaded BALB/c and C57BL/6 cells but interrupted if the donor cells were pretreated with anti-CD62L antibody (Fig. 7; Fig. 8B, part 3). We suggest that the L-selectin-dependent leukocyte-mediated Trojan horse commonly appears in both mouse strains and that the Ly6C⁺CD62L⁺GFP⁺ inflamed cells are the best candidate for the Trojan horse.

However, several lines of research indicated that the infected CD62L⁺Ly6C⁺ cells were not the only likely Trojan horse. For example, a low but significant proportion (5.5%; 2/36) of *sell*^{-/-} KO mice still developed neurologic melioidosis after intravenous infection with *B. pseudomallei* (5×10^5 CFU) (data not shown). *B. pseudomallei* can also persist in non-phagocytic cells that readily migrate in the BM, such as lymphoid lineage CD11b⁺CD150⁺ cells (Fig. 5C), and CD19 (B cell) antigens are expressed in BILs (data not shown). Moreover, a low level of bacteria colonizing the brain was induced in the recipient mice after adoptive transfer of *B. pseudomallei*-loaded *sell*^{-/-} Ly6C cells.

In summary, our results suggest that the Ly6C⁺CD62L⁺ leukocytes are an important Trojan horse in the development of neurologic melioidosis. The leukocytic L-selectin should not simply be considered as a temporally elicited antigen but rather as a lineage differentiation marker during spreading and infection of melioidosis in animal and/or human brains.

Disclosure of potential conflicts of interest

No potential conflicts of interest were disclosed.

Funding

This project was supported by MOST (Ministry of Science and Technology, ROC) grants (NSC102-2628-B-075B-002-MY3 [Chen, YL]; MOST103-2320-B-017-001 [Chen, YL];

MOST103-2320-B-075B-002 [Chen YS]; and MOST103-2320-B-214-008 [Lin, HH]) and by Kaohsiung Veterans General Hospital (VGH-KS) grants (VGHKS102-016, VGHKS103-055 and VGHKS104-061 [Chen, YS]).

ORCID

Ya-Lei Chen  <http://orcid.org/0000-0003-0893-955X>

References

- [1] Cheng AC, Currie BJ. Melioidosis: epidemiology, pathophysiology, and management. *Clin Microbiol Rev* 2005; 18:383-416; PMID:15831829; <https://doi.org/10.1128/CMR.18.2.383-416.2005>
- [2] Dance DA. Ecology of *Burkholderia pseudomallei* and the interactions between environmental *Burkholderia spp.* and human-animal hosts. *Acta Trop* 2000; 74:159-68; PMID:10674645; [https://doi.org/10.1016/S0001-706X\(99\)00066-2](https://doi.org/10.1016/S0001-706X(99)00066-2)
- [3] Cheng AC. Melioidosis: advances in diagnosis and treatment. *Curr Opin Infect Dis* 2010; 23:554-9; PMID:20847695; <https://doi.org/10.1097/QCO.0b013e32833fb88c>
- [4] Muttarak M, Peh WC, Euathrongchit J, Lin SE, Tan AG, Lerttumnongtum P, Sivasomboon C. Spectrum of imaging findings in melioidosis. *Br J Radiol* 2009; 82:514-21; PMID:19098086; <https://doi.org/10.1259/bjr/15785231>
- [5] Jabbar Z, Currie BJ. Melioidosis and the kidney. *Nephrology (Carlton, Vic)* 2013; 18:169-75; PMID:23279670
- [6] Meumann EM, Cheng AC, Ward L, Currie BJ. Clinical features and epidemiology of melioidosis pneumonia: results from a 21-year study and review of the literature. *Clin Infect Dis* 2012; 54:362-9; PMID:22057702; <https://doi.org/10.1093/cid/cir808>
- [7] Currie BJ, Fisher DA, Howard DM, Burrow JN. Neurologic melioidosis. *Acta trop* 2000; 74:145-51; PMID:10674643; [https://doi.org/10.1016/S0001-706X\(99\)00064-9](https://doi.org/10.1016/S0001-706X(99)00064-9)
- [8] Owen SJ, Batzloff M, Chehrehasa F, Meedeniya A, Casart Y, Logue CA, Hirst RG, Peak IR, Mackay-Sim A, Beacham IR. Nasal-associated lymphoid tissue and olfactory epithelium as portals of entry for *Burkholderia pseudomallei* in murine melioidosis. *J Infect Dis* 2009; 199:1761-70; PMID:19456230; <https://doi.org/10.1086/599210>
- [9] St John JA, Ekberg JA, Dando SJ, Meedeniya AC, Horton RE, Batzloff M, Owen SJ, Holt S, Peak IR, Ulett GC, et al. *Burkholderia pseudomallei* penetrates the brain via destruction of the olfactory and trigeminal nerves: implications for the pathogenesis of neurologic melioidosis. *mBio* 2014; 5:e00025; PMID:24736221
- [10] White NJ. Melioidosis. *Lancet* 2003; 361:1715-22; PMID:12767750; [https://doi.org/10.1016/S0140-6736\(03\)13374-0](https://doi.org/10.1016/S0140-6736(03)13374-0)
- [11] Weiss N, Miller F, Cazaubon S, Couraud PO. The blood-brain barrier in brain homeostasis and neurologic diseases. *Biochim Biophys Acta* 2009; 1788:842-57; PMID:19061857; <https://doi.org/10.1016/j.bbame.2008.10.022>
- [12] Barnes JL, Ulett GC, Ketheesan N, Clair T, Summers PM, Hirst RG. Induction of multiple chemokine and colony-stimulating factor genes in experimental *Burkholderia pseudomallei* infection. *Immunol Cell Biol* 2001; 79:490-501; PMID:11564157; <https://doi.org/10.1046/j.1440-1711.2001.01038.x>
- [13] Conejero L, Patel N, de Reynal M, Oberdorf S, Prior J, Felgner PL, Titball RW, Salguero FJ, Bancroft GJ. Low-dose exposure of C57BL/6 mice to *Burkholderia pseudomallei* mimics chronic human melioidosis. *Am J Pathol* 2011; 179:270-80; PMID:21703409; <https://doi.org/10.1016/j.ajpath.2011.03.031>
- [14] West TE, Myers ND, Limmathurotsakul D, Liggitt HD, Chantratita N, Peacock SJ, Skerrett SJ. Pathogenicity of high-dose enteral inoculation of *Burkholderia pseudomallei* to mice. *Am J Trop Med Hyg* 2010; 83:1066-9; PMID:21036839; <https://doi.org/10.4269/ajtmh.2010.10-0306>
- [15] West TE, Myers ND, Liggitt HD, Skerrett SJ. Murine pulmonary infection and inflammation induced by inhalation of *Burkholderia pseudomallei*. *Int J Exp Pathol* 2012; 93:421-8; PMID:23136994; <https://doi.org/10.1111/j.1365-2613.2012.00842.x>
- [16] Goodyear A, Bielefeldt-Ohmann H, Schweizer H, Dow S. Persistent gastric colonization with *Burkholderia pseudomallei* and dissemination from the gastrointestinal tract following mucosal inoculation of mice. *PloS One* 2012; 7:e37324; PMID:22624016; <https://doi.org/10.1371/journal.pone.0037324>
- [17] Williams NL, Kloeze E, Govan BL, Korner H, Ketheesan N. *Burkholderia pseudomallei* enhances maturation of bone marrow-derived dendritic cells. *Trans R Soc Trop Med Hyg* 2008; 102(Suppl 1):S71-5; PMID:19121693; [https://doi.org/10.1016/S0035-9203\(08\)70019-1](https://doi.org/10.1016/S0035-9203(08)70019-1)
- [18] Williams NL, Morris JL, Rush CM, Ketheesan N. Migration of dendritic cells facilitates systemic dissemination of *Burkholderia pseudomallei*. *Infect Immun* 2014; 82:4233-40; PMID:25069976; <https://doi.org/10.1128/IAI.01880-14>
- [19] Morris J, Fane A, Rush C, Govan B, Mayo M, Currie BJ, Ketheesan N. Neurotropic threat characterization of *Burkholderia pseudomallei* strains. *Emerg Infect Dis* 2015; 21:58-63; PMID:25530166; <https://doi.org/10.3201/eid2101.131570>
- [20] Liu PJ, Chen YS, Lin HH, Ni WF, Hsieh TH, Chen HT, Chen YL. Induction of mouse melioidosis with meningitis by CD11b+ phagocytic cells harboring intracellular *B. pseudomallei* as a Trojan horse. *PLoS Negl Trop Dis* 2013; 7:e2363; PMID:23951382; <https://doi.org/10.1371/journal.pntd.0002363>
- [21] Zarbock A, Ley K, McEver RP, Hidalgo A. Leukocyte ligands for endothelial selectins: specialized glycoconjugates that mediate rolling and signaling under flow. *Blood* 2011; 118:6743-51; PMID:22021370; <https://doi.org/10.1182/blood-2011-07-343566>
- [22] Engelhardt B. Immune cell entry into the central nervous system: involvement of adhesion molecules and chemokines. *J Neurol Sci* 2008; 274:23-6; PMID:18573502; <https://doi.org/10.1016/j.jns.2008.05.019>
- [23] Arbones ML, Ord DC, Ley K, Ratech H, Maynard-Curry C, Otten G, Capon DJ, Tedder TF. Lymphocyte homing and leukocyte rolling and migration are impaired in L-selectin-

- deficient mice. *Immunity* 1994; 1:247-60; PMID:7534203; [https://doi.org/10.1016/1074-7613\(94\)90076-0](https://doi.org/10.1016/1074-7613(94)90076-0)
- [24] Angiari S, Constantin G. Selectins and their ligands as potential immunotherapeutic targets in neurologic diseases. *Immunotherapy* 2013; 5:1207-20; PMID:24188675; <https://doi.org/10.2217/imt.13.122>
- [25] Gordon S, Taylor PR. Monocyte and macrophage heterogeneity. *Nature Rev Immunol* 2005; 5:953-64; <https://doi.org/10.1038/nri1733>
- [26] Chen YS, Lin HH, Hsueh PT, Liu PJ, Ni WF, Chung WC, Lin CP, Chen YL. Whole-Genome Sequence of an Epidemic Strain of *Burkholderia pseudomallei* vgh07 in Taiwan. *Genome announc* 2015; 3:pii: e00345-15; PMID:25931599
- [27] Alexeyev MF. The pKNOCK series of broad-host-range mobilizable suicide vectors for gene knockout and targeted DNA insertion into the chromosome of gram-negative bacteria. *BioTechniques* 1999; 26:824-6; PMID:10337469
- [28] Carvalho LP, Petritus PM, Trochtenberg AL, Zaph C, Hill DA, Artis D, Scott P. Lymph node hypertrophy following Leishmania major infection is dependent on TLR9. *J Immunol*. 2012; 188:1394-401; PMID:22205030; <https://doi.org/10.4049/jimmunol.1101018>
- [29] Huang HS, Sun DS, Lien TS, Chang HH. Dendritic cells modulate platelet activity in IVIg-mediated amelioration of ITP in mice. *Blood* 2010; 116:5002-9; PMID:20699442; <https://doi.org/10.1182/blood-2010-03-275123>
- [30] Pascual DW, Riccardi C, Csencsits-Smith K. Distal IgA immunity can be sustained by alphaEbeta7+ B cells in L-selectin^{-/-} mice following oral immunization. *Mucosal Immunol* 2008; 1:68-77; PMID:19079162; <https://doi.org/10.1038/mi.2007.2>
- [31] Sun DS, Chang YC, Lien TS, King CC, Shih YL, Huang HS, Wang TY, Li CR, Lee CC, Hsu PN, et al. Endothelial cell Sensitization by death receptor fractions of an anti-dengue monstructural protein 1 antibody induced plasma leakage, coagulopathy, and mortality in Mice. *J Immunol* 2015; 195:2743-53; PMID:26259584; <https://doi.org/10.4049/jimmunol.1500136>
- [32] Harry GJ, Kraft AD. Microglia in the developing brain: a potential target with lifetime effects. *Neurotoxicology* 2012; 33:191-206; PMID:22322212; <https://doi.org/10.1016/j.neuro.2012.01.012>
- [33] Chen YS, Shieh WJ, Goldsmith CS, Metcalfe MG, Greer PW, Zaki SR, Chang HH, Chan H, Chen YL. Alteration of the phenotypic and pathogenic patterns of *Burkholderia pseudomallei* that persist in a soil environment. *Am J Trop Med Hyg* 2014; 90:469-79; PMID:24445207; <https://doi.org/10.4269/ajtmh.13-0051>
- [34] Stevens MP, Wood MW, Taylor LA, Monaghan P, Hawes P, Jones PW, Wallis TS, Galyov EE. An Inv/Mxi-Spa-like type III protein secretion system in *Burkholderia pseudomallei* modulates intracellular behaviour of the pathogen. *Mol Microbiol* 2002; 46:649-59; PMID:12410823; <https://doi.org/10.1046/j.1365-2958.2002.03190.x>
- [35] Stevens MP, Haque A, Atkins T, Hill J, Wood MW, Easton A, Nelson M, Underwood-Fowler C, Titball RW, Bancroft GJ, et al. Attenuated virulence and protective efficacy of a *Burkholderia pseudomallei* bsa type III secretion mutant in murine models of melioidosis. *Microbiol* 2004; 50(Pt 8):2669-76; <https://doi.org/10.1099/mic.0.27146-0>
- [36] Ulett GC, Ketheesan N, Hirst RG. Cytokine gene expression in innately susceptible BALB/c mice and relatively resistant C57BL/6 mice during infection with virulent *Burkholderia pseudomallei*. *Infect Immun* 2000; 68:2034-42; PMID:10722599; <https://doi.org/10.1128/IAI.68.4.2034-2042.2000>
- [37] Liu B, Koo GC, Yap EH, Chua KL, Gan YH. Model of differential susceptibility to mucosal *Burkholderia pseudomallei* infection. *Infect Immun* 2002; 70:504-511; PMID:11796576; <https://doi.org/10.1128/IAI.70.2.504-511.2002>
- [38] Tan GY, Liu Y, Sivalingam SP, Sim SH, Wang D, Paucod JC, Gauthier Y, Ooi EE. *Burkholderia pseudomallei* aerosol infection results in differential inflammatory responses in BALB/c and C57BL/6 mice. *J Med Microbiol* 2008; 57:508-515; PMID:18349373; <https://doi.org/10.1099/jmm.0.47596-0>
- [39] Chieng S, Carreto L, Nathan S. *Burkholderia pseudomallei* transcriptional adaptation in macrophages. *BMC Genomics* 2012; 13:328; PMID:22823543; <https://doi.org/10.1186/1471-2164-13-328>
- [40] Tuanyok A, Tom M, Dunbar J, Woods DE. Genome-wide expression analysis of *Burkholderia pseudomallei* infection in a hamster model of acute melioidosis. *Infect Immun* 2006; 74:5465-5476; PMID:16988221; <https://doi.org/10.1128/IAI.00737-06>
- [41] Eske K, Breitbach K, Kohler J, Wongprompitak P, Steinmetz I. Generation of murine bone marrow derived macrophages in a standardised serum-free cell culture system. *J Immunol Methods* 2009; 342:13-9; PMID:19133267; <https://doi.org/10.1016/j.jim.2008.11.011>
- [42] Santos JL, Andrade AA, Dias AA, Bonjardim CA, Reis LF, Teixeira SM, Horta MF. Differential sensitivity of C57BL/6 (M-1) and BALB/c (M-2) macrophages to the stimuli of IFN-gamma/LPS for the production of NO: correlation with iNOS mRNA and protein expression. *J Interferon Cytokine Res*. 2006; 26:682-8; PMID:16978073; <https://doi.org/10.1089/jir.2006.26.682>
- [43] Breitbach K, Klocke S, Tschernig T, van Rooijen N, Baumann U, Steinmetz I. Role of inducible nitric oxide synthase and NADPH oxidase in early control of *Burkholderia pseudomallei* infection in mice. *Infect Immun* 2006; 74:6300-9; PMID:17000727; <https://doi.org/10.1128/IAI.00966-06>
- [44] Depke M, Breitbach K, Dinh Hoang Dang K, Brinkmann L, Salazar MG, Dhople VM, Bast A, Steil L, Schmidt F, Steinmetz I, et al. Bone marrow-derived macrophages from BALB/c and C57BL/6 mice fundamentally differ in their respiratory chain complex proteins, lysosomal enzymes and components of antioxidant stress systems. *J Proteomics* 2014; 103:72-86; PMID:24704164; <https://doi.org/10.1016/j.jprot.2014.03.027>
- [45] Guillemin GJ, Brew BJ. Microglia, macrophages, perivascular macrophages, and pericytes: a review of function and identification. *J Leukoc Biol* 2004; 75:388-97; PMID:14612429; <https://doi.org/10.1189/jlb.0303114>
- [46] Rock RB, Gekker G, Hu S, Sheng WS, Cheeran M, Lokensgard JR, Peterson PK. Role of microglia in central nervous system infections. *Clin Microbiol Rev* 2004; 17:942-64; PMID:15489356; <https://doi.org/10.1128/CMR.17.4.942-964.2004>

- [47] Utaisincharoen P, Tangthawornchaikul N, Kespichayawattana W, Anuntagool N, Chaisuriya P, Sirisinha S. Kinetic studies of the production of nitric oxide (NO) and tumour necrosis factor- α (TNF- α) in macrophages stimulated with *Burkholderia pseudomallei* endotoxin. *Clin Exp Immunol* 2000; 122:324-9; PMID:11122236; <https://doi.org/10.1046/j.1365-2249.2000.01386.x>
- [48] Yao Y, Tsirka SE. Monocyte chemoattractant protein-1 and the blood-brain barrier. *Cell Mol Life Sci* 2014; 71:683-97; PMID:24051980; <https://doi.org/10.1007/s00018-013-1459-1>
- [49] Menetski J, Mistry S, Lu M, Mudgett JS, Ransohoff RM, Demartino JA, Macintyre DE, Abbadie C. Mice overexpressing chemokine ligand 2 (CCL2) in astrocytes display enhanced nociceptive responses. *Neuroscience* 2007; 149:706-14; PMID:17870246; <https://doi.org/10.1016/j.neuroscience.2007.08.014>
- [50] Getts DR, Terry RL, Getts MT, Muller M, Rana S, Shrestha B, Radford J, Van Rooijen N, Campbell IL, King NJ. 2008. Ly6c+ “inflammatory monocytes” are microglial precursors recruited in a pathogenic manner in West Nile virus encephalitis. *J Exp Med* 2008; 205:2319-37; PMID:18779347; <https://doi.org/10.1084/jem.20080421>
- [51] Guilliams M, Lambrecht BN, Hammad H. Division of labor between lung dendritic cells and macrophages in the defense against pulmonary infections. *Mucosal Immunol*. 2013; 6:464-73; PMID:23549447; <https://doi.org/10.1038/mi.2013.14>
- [52] Chen YS, Shiuan D, Chen SC, Chye SM, Chen YL. Recombinant truncated flagellin of *Burkholderia pseudomallei* as a molecular probe for diagnosis of melioidosis. *Clin Diagn Lab Immunol* 2003; 10:423-5; PMID:12738642